coatings

MDPI

*Article*

# Optimization of Lost Foam Coating Performance: Effects of Blade Shape, Stirring Speed, and Drying Temperature on Viscosity, Coating Weight, and Surface Morphology

**Guojin Sun [1,*], Zhenggui Li [1] and Qi Wang [2]**

[1] School of Engineering, Qinghai Institute of Technology, Xining 810016, China; lzhgui@mail.xhu.edu.cn
[2] Electrical Engineering Division, Department of Engineering, University of Cambridge, Cambridge CB3 0FA, UK; qw273@cam.ac.uk
* Correspondence: guojinsun@qhit.edu.cn

**Abstract:** The current investigation focuses on the viscosity, coating weight, and surface characteristics of lost foam casting coatings, examining the effects of blade shape, stirring speed, and stirring time. A systematic analysis was conducted to determine how different stirring speeds and durations influenced coating weight and viscosity. The results indicate that the blade shape has a considerable impact on the uniformity and efficacy of the coating, with some designs being far more effective in reaching the optimal viscosity and coating weight through uniformly distributed mixing. Results were consistently obtained when stirring at 800–1200 rpm. It was demonstrated that while stirring speed significantly impacts coating deposition, it has small effect on viscosity. A stirring time of 30 min was found optimal for stabilizing coating weight and viscosity without significant variations. Drying at room temperature produced smoother surfaces with fewer cracks, whereas higher drying temperatures (50 °C) were associated with increased surface roughness and cracking. Crack analysis after drying revealed that coatings mixed with the tri-blade had the lowest tendency to crack, demonstrating its superior capability for even and thorough mixing.

**Keywords:** lost foam coatings; blade shape; viscosity; coating weight; surface morphology; drying behavior



**Citation:** Sun, G.; Li, Z.; Wang, Q. Optimization of Lost Foam Coating Performance: Effects of Blade Shape, Stirring Speed, and Drying Temperature on Viscosity, Coating Weight, and Surface Morphology. *Coatings* **2024**, *14*, 1106. https://doi.org/10.3390/coatings14091106

Academic Editor: Alexander Tolstoguzov

Received: 26 July 2024
Revised: 21 August 2024
Accepted: 23 August 2024
Published: 2 September 2024



## 1. Introduction

Boasting a history spanning over thirty years of existence, lost foam casting is acknowledged as a notable casting technique of the twenty-first century. This technique can produce castings with smooth surfaces and accurate dimensions, which makes it easy to mechanize the manufacturing procedure followed by significantly reduces production costs [1–3]. It provides a great deal of design flexibility, which boosts production effectiveness and makes clean production possible to achieve casting that is both economical and ecologically friendly [4,5]. A great deal of domestic companies have currently embraced cutting-edge machinery and procedures to fulfill the demands for manufacturing castings made of a variety of materials. Lost foam casting, also known as evaporative pattern casting, involves the use of a foam pattern that evaporates when in contact with molten metal, leaving behind a precisely shaped casting [6–10]. Simply by doing away with conventional cores and parting lines, the method can lower flaws and raise the overall caliber of the castings. This process is very useful for creating intricate geometries that would be challenging to achieve utilizing conventional casting forms of payment.

In the lost foam casting process, the coating is a crucial technology. Reviewing the development of this process reveals the increasingly prominent role of lost foam casting coatings. In recent years, numerous scholars have identified lost foam casting coatings as one of the three main research focuses for the further development and application of this technology [11–16]. Additionally, scholars have emphasized the importance of coatings in

process control. The functions of lost foam coatings include supporting and protecting the foam model, preventing liquid metal from infiltrating the sand and adhering to the sand, absorbing decomposition products, and allowing decomposition gases to pass through the coating [17,18]. When the foam mold breaks, it helps maintain the integrity of the cavity's air while preventing the rapid loss of heat from the liquid metal. Therefore, lost foam coatings must have sufficient refractoriness, appropriate mechanical strength, suitable thermal insulation and conductivity, appropriate permeability and absorption capacity for liquid decomposition products, a smooth surface, adequate brushing performance, and must not chemically react with the foam model [19–21]. Those properties are necessary in order to ensure that the coating successfully carries out its protective and supporting functions during the casting process. Developments in materials science have made it easier to create coatings with enhanced characteristics, which has contributed to better performance and expanded the use of lost foam casting.

The casting process technology has developed substantially in recent years, which has increased coating variations, broadening coating functionality, in addition to improving decorating performance even further. Ensuring the production of casting products of superior quality requires the appropriate selection and application of coatings. Due to the complexity of coating compositions and their critical role in the casting process, the selection of coatings and the success of the EPC (Expendable Pattern Casting) process are vital, necessitating ongoing performance analysis and measurement of the coatings, particularly their viscosity, coating weight, and surface morphology. These parameters significantly impact the final quality of the castings and the efficiency of the production process [22,23]. Indeed, coatings are essential to producing castings of superior quality. Enhancing coating performance greatly raises the likelihood of successful castings in the lost foam casting process, as production and research have demonstrated [24–26]. Our understanding of the connection between the technological procedures used in coating development and their mechanical characteristics has greatly improved as a result of earlier studies. Research on coatings' chemical makeup has typically focused on how changes in binders, additives, and other chemical components impact properties like adhesion, durability, and viscosity. For example, Pimenta et al. investigated how varying binder concentrations influence the performance characteristics of intumescent coatings [27–29], and Sun et al. examined wettability throughout the entire filling process [30–33]. However, these studies frequently overlooked the critical influence of mechanical factors, such as stirring speed, blade shape, and mixing time—factors that significantly impact the rheological properties and coating application quality.

By focusing on the mechanical aspects of coating preparation and examining the effects of stirring speed, duration, and blade shape on the effectiveness of dispersed foam protective coatings, this work establishes a new standard in the industry. Unlike earlier research that primarily focused specifically on the compositions of chemical compounds, this study highlights the significance of physical production methods. It illustrates how fine surveillance over technological variables may greatly improve coatings' rheological properties and surface morphology. This research is noteworthy for its thorough analysis of the relationship between mechanical stirring and coating behavior. These insights have the potential to greatly enhance the process of preparing lost foam coatings. This study advances the field of casting techniques by providing accurate guidelines for improving the preparation of high-performance coatings, effectively bridging the gap between theory and practice.

## 2. Materials and Methods

### *2.1. Experimental Materials*

Professional lost foam casting coatings were the components that were employed in the present research. These coatings are capable of being used in a variety of industries due to their high layer strength and great permeability. The finished product has a great coverage and is simple to apply. The coating utilized in this investigation is a precisely

calculated blend of refreshments and powders believed to have been well mixed before application. $Al_2O_3$ and $SiO_2$ are the primary refractory fillers in the powder component, with average particle sizes fluctuating between 300 to 800 µm. Iron oxide powder, sodium carboxymethyl cellulose (SN thickener), and sodium bentonite are also included in trace amounts. The liquid component is a water-based solution that contains SN thickener and latex. It has a density of 1.2 g/cm$^3$ and a pH of 8–9.

A ratio of 1.25:1, or 250 g of coating powders to 200 g weight of water, was used to prepare the coating solution. To ensure thorough mixing, the slurry was further processed with a high-speed disperser, as illustrated in Figure 1. The study conducted here chose a number of blade types, including serrated-blade, straight-blade, tri-blade, and quad-blade, to examine the consequences of various blade shapes on the functioning of the coatings. The stirring blades were made from 1.5 mm thick stainless steel with a surface finish of no less than 1.0 µm. Table 1 provides a summary of the characteristics of the different stirring blades used in this study to give a clear understanding of the equipment employed.

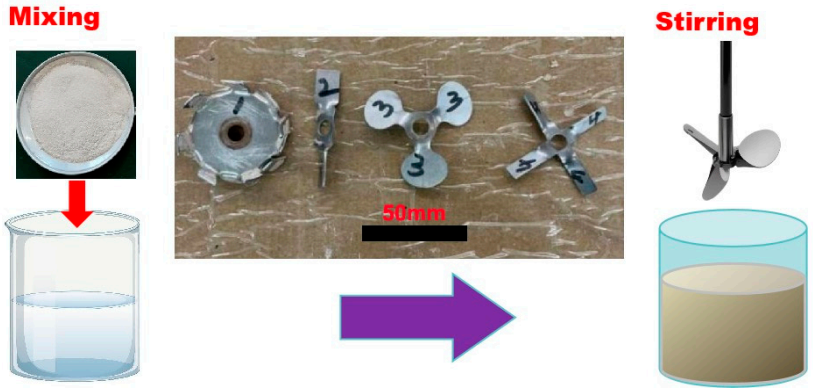


**Figure 1.** Schematic diagram of coating preparation process.

**Table 1.** Characteristics of stirring blades used in the study.

| Blade Type | Blade Shape | Application Scope and Characteristics |
|---|---|---|
| Blade1 | serrated<br>50 mm × 1.5 mm | Commonly used for high-speed shearing and dispersion, effectively dispersing pigments, powders, and other materials evenly. |
| Blade2 | straight<br>50 mm × 1.5 mm | Primarily used for fluid circulation or stirring high-viscosity materials, with limited axial flow range. |
| Blade3 | tri<br>50 mm × 1.5 mm | Draws fluid from above the blades, creating axial flow. Turbulence is minimal during mixing, but circulation is extensive. Provides less shear but excellent top-to-bottom mixing. |
| Blade4 | quad<br>50 mm × 1.5 mm | Ideal for high-speed shearing and dispersion, efficiently dispersing pigments, powders, and other materials evenly. |

### *2.2. Coating Physical Property Measurements*

Measuring the viscosity of cast coating is crucial for precisely predicting and controlling the coating's performance during application. A Shanghai Fangriu Instrument Co., Ltd. China, rotational viscometer was used in this study to assess the uniformity of the highlighting coatings applied. The viscosity is evaluated at three separate spots at the same rotating speed to confirm the correctness of the experimental data, and the average value is used to determine the viscosity of the casting coating. Rotor No. 3 was selected, and the rotor's rotational speed is set at 6, 12, 30, and 60 rpm, respectively. In order to guarantee information accuracy among samples, it is crucial to reduce the time gap between the technique of sampling and measurements because the coating's viscosity steadily increases once the swirled coating is allowed to stand. Every testing procedure was performed out at room temperature, or roughly 20 °C. The research project not only evaluated viscosity

at various rotational speeds but also took the coatings' thixotropic behavior into account. The rheological properties of the lost foam coatings, including apparent viscosity, were analyzed to gain insights into their performance during application.

The coating weight was measured using metal sheets with dimensions of 40 mm × 40 mm × 2 mm. First, the metal sheet was tared and weighed using an electronic balance. Then, the sheet was fully immersed in the coating solution for two minutes and taken out from the coating solution. Subsequently, the coating either ceased to moves completely or dripped very slowly, and the electronic weighing device was used to weigh the metal sheet once more. The relative coating weight is represented by the weight difference between the pre- and post-immersion values. For the purposes of accuracy, the above procedure was carried out approximately at three different times for each sample, and the average value was noted.

### *2.3. Analysis of the Coating Drying Process*

Individual stirred coating slurry was gradually poured into molds spanning approximately 40 mm in diameter and 2 mm in depth in order to investigate the procedure for the drying of the coatings. After that, the coatings were dried in an oven set at a constant temperature. To examine the drying process under different circumstances, the weight of the coatings was measured on a regular basis. The XMTA-6000 constant temperature oven (Shanghai Yatai Instrument Co., Ltd., Shanghai, China) was chosen in this study. The samples were dried at temperatures of 30, 40, and 50 °C during the drying process examination. To guarantee uniform drying conditions of use, the oven was warmed to the necessary temperature before each drying cycle. To achieve even drying, the samples were positioned in the center of the oven. Each sample was carefully prepared to ensure uniform thickness and volume, minimizing variability in the drying process.

## 3. Results and Discussion

### *3.1. Influence of Blade Shape on Coating Performance*

The variations in the forms of the stirring blades used to stir the coating can lead to different levels of homogeneity, which can impact the coating's effectiveness. To analyze the influence of blade shape on the performance of the coating after stirring, the stirring speed was fixed at 1000 rpm, and the stirring time was set to 30 min. The results are shown in Figure 2.

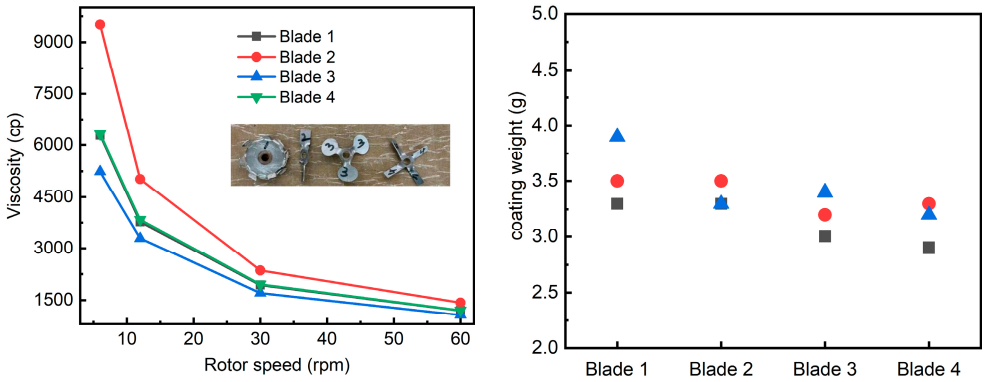


(**a**) Variation in coating viscosity (**b**) Variation in coating weight

**Figure 2.** Effect of blade shape on coating viscosity and coating weight.

As seen in Figure 2a, changing the blade shape leads to different coating viscosities under the same stirring speed and time. At a constant rotor speed, the viscosity of the solution stirred by Blade 2 is the highest, while the viscosities of the solutions stirred by Blades 1 and 4 are similar, both being lower than that stirred by Blade 2. The solution stirred by Blade 3 has the lowest viscosity. This can be attributed to the shear thinning

characteristic of the lost foam coating, where the viscosity decreases with increased stirring intensity. The viscosity measurements in Figure 2 indicate that Blade 2 has the weakest stirring ability; achieving the same mixing effect would require a longer stirring time or higher stirring speed. Blade 4 shows the strongest stirring ability, quickly achieving uniform mixing. The coating weight also varies with different blade shapes, with Blade 4 resulting in the lowest coating weight and Blade 1 the highest, consistent with the viscosity results. In general, Blade 3 has the best mixing capability, making it the preferred choice for complete and effective mixing.

The observed differences in viscosity indicate that blade shape significantly influences the mixing efficiency and coating quality. Blade 3, with its superior mixing capability, ensures a more uniform and consistent coating, which is crucial for achieving high-quality castings with minimal defects. The outcomes establish how crucial it is to make decisions about the best possible blade shape in order to achieve highest coating efficiency and improve the quality and functionality of completed cast objects. The insights gained from this analysis provide valuable guidelines for improving the efficiency and quality of the coating process in industrial applications, contributing to advancements in casting technology.

### *3.2. Influence of Stirring Speed on Coating Performance*

Understanding the connection that exists between stirring speed and coating properties is essential to ensuring optimal coating performance. Blade 3 was selected for this study in order to learn about the effects of stirring speed on coating performance, and a stirring duration of 30 min was established. The effect of stirring speed on coating viscosity and coating weight are shown in Figure 3.

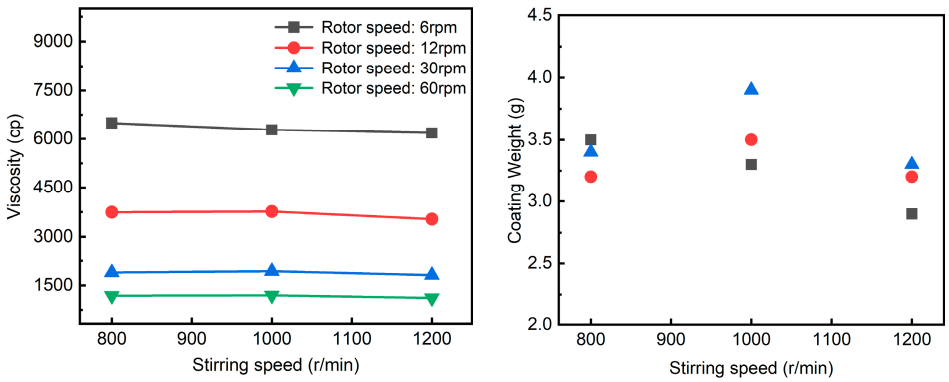


(**a**) Variation in coating viscosity (**b**) Variation in coating weight

**Figure 3.** Effect of stirring speed on coating viscosity and coating weight.

From Figure 3a, it can be seen that the viscosity of the coating shows a slight decrease with increasing stirring speed, although the overall change is not significant. This shows that after a 30 min period of stirring, the coating reaches homogeneity at the designated stirring speeds of 800–1200 rpm. As Figure 3b illustrates, the coating weight is somewhat less at 1200 rpm of stirring than it is at 800 rpm and 1000 rpm. Shear thinning, in which the coating's viscosity reduces at higher shear rates and results in a reduced coating thickness, is the root cause of this coating weight reduction at 1200 rpm.

The research results demonstrate that stirring at a speed between 800–1200 rpm works well to create a uniform coating mixture. For some uses that need thinner coatings, the minor decrease in viscosity and coating weight at faster speeds can be beneficial to use. These findings underscore the importance of optimizing stirring speed to enhance the coating performance, ensuring consistent quality and optimal properties for lost foam casting processes. The insights from this study offer helpful recommendations for industrial use that promote the choice of suitable stirring parameters to provide the required coating characteristics.

### *3.3. Influence of Stirring Time on Coating Performance*

The duration of stirring time chosen in producing lost foam coatings has an impact on the coating's performance. On average, too little stirring time may outcome in poor mixing, while too much stirring time can raise expenditures and waste. This work uses Blade 3 and a stirring rate of 800 rpm to consider the effect of stirring time on coating performance. The effects of stirring time on coating viscosity and coating weight are illustrated in Figure 4.

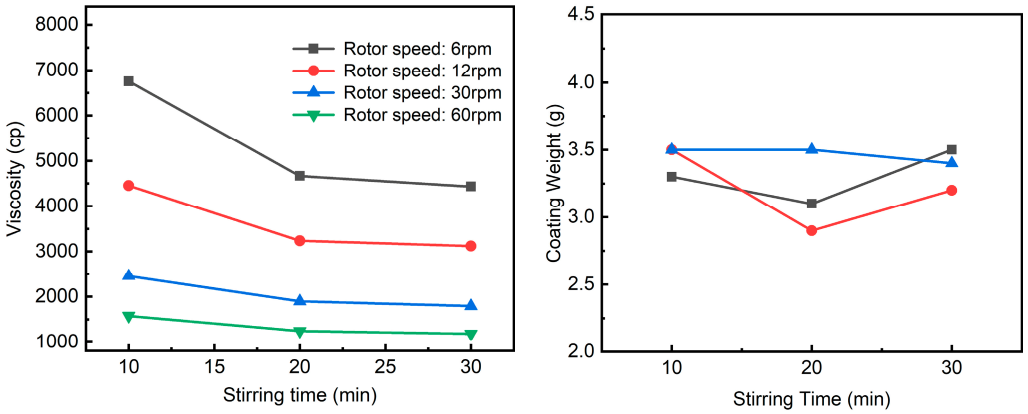


(**a**) Variation in coating viscosity (**b**) Variation in coating weight

**Figure 4.** Effect of stirring time on coating viscosity and coating weight.

As depicted in Figure 4a, with a constant stirring speed of 800 rpm and consistent blade shape, the viscosity of the coating exhibits a slight decreasing trend as the stirring time increases. After a significant amount of stirring time, the viscosity quickly stabilizes, suggesting that additional stirring time increases have a limited impact on viscosity. As can be seen in Figure 4b, the coating weight is marginally higher than average after 10 min of stirring, it is lower than average after 20 min, and it is closer to the average value after 30 min. However, the differences in stirring time do not result in significant changes in coating weight, which remains within a small range of fluctuation. Therefore, once the coating achieves a stable viscosity and coating weight after a certain stirring period, extending the stirring time further has minimal impact on coating performance.

In conclusion, the weight and viscosity of the coating stay essentially unchanged when the stirring time is increased beyond a certain point. This result emphasizes how important it is to stir for an appropriate amount of time to achieve uniform coating qualities without wasting money or resources. These insights are helpful in ensuring the effectiveness and efficiency of coating performance in industrial applications through efficiencies in the preparation rules and regulations.

### *3.4. Analysis of Coating Drying Behavior*

After the coating is prepared and mixed, it is applied to the model surface and subsequently dried to achieve a certain strength and maintain a specific shape. The performance of the coating can be significantly impacted by improper choice of drying settings, which can result in flaws such cracking, distortion, and insufficient strength during the drying process. The coatings that had been combined with various blade forms were dried at 30, 40, and 50 °C. The surface morphology of the fully dried coatings is shown in Figure 5.

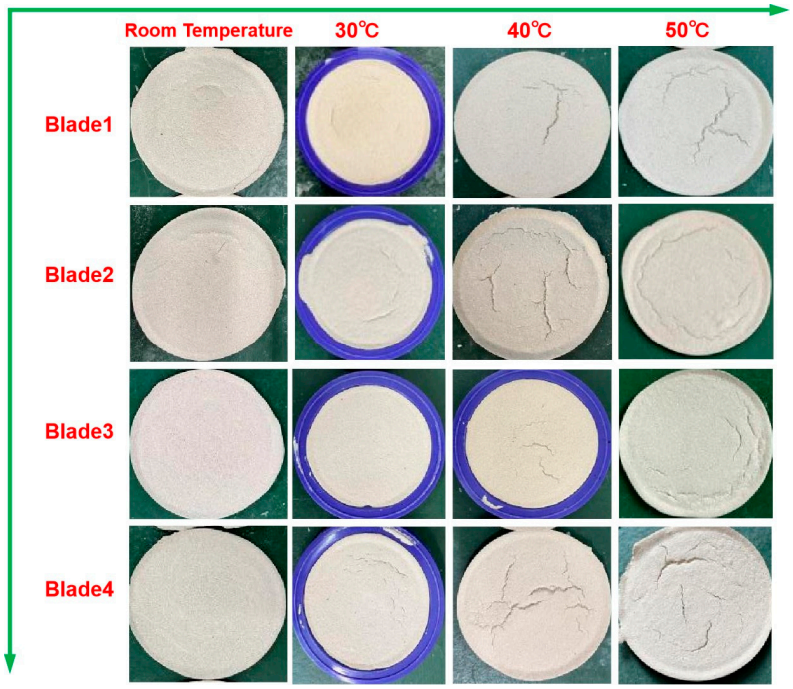


**Figure 5.** Coating macroscopic morphology.

Based on the surface morphology of the fully dried coatings stirred by different blades, as shown in Figure 5, it can be observed that higher drying temperatures result in more pronounced surface cracks and rougher surface textures. Coatings including all four blade types show comparatively smooth outer layers at room temperature. At 30 °C, slight cracks are observed on the surfaces of all four coatings, with the coating mixed with Blade 3 being the smoothest. At 40 °C, more noticeable cracks appear on the surfaces of all coatings. The coatings mixed with Blade 1 and 3 shows relatively fewer cracks compared to those mixed with Blades 2 and 4. At 50 °C, the surfaces of the coatings show very prominent cracks, with the coating mixed with Blade 3 exhibiting fewer cracks compared to those mixed with other blades.

To further analyze the effects of blade shape and drying temperature on surface cracking of the coating, we conducted a quantitative analysis of the cracks. The total crack length for each sample was measured (in pixel units, px), with the results presented in Figure 6.

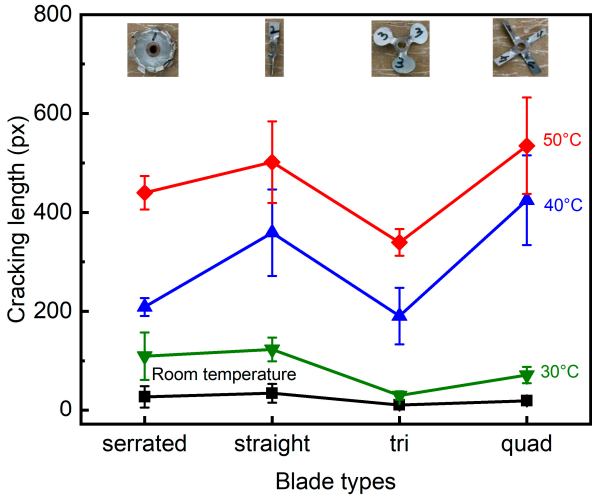


**Figure 6.** Analysis of the effect of blade type on surface crack formation in the coatings.

The results of this study, as shown in Figure 6, clearly demonstrate that the tendency for cracks to appear on the coating surface increases with the drying temperature. Compared to the other four blade types tested, the coating mixed with Blade 3 consistently exhibited shorter crack lengths across all drying temperatures. This indicates that the mixing procedure with Blade 3 is more efficient and consistent. Furthermore, the coatings mixed with Blade 3 not only had shorter crack lengths but also displayed noticeably less variability in crack sizes. Based on the frequency of cracks observed under different drying conditions, Blade 3 produced a more homogeneous and well-mixed coating compared to the other blades.

Figure 7 presents the weight curves for coatings dried at different temperatures. Each curve demonstrates the weight loss trend as a function of time for coatings subjected to various drying conditions.

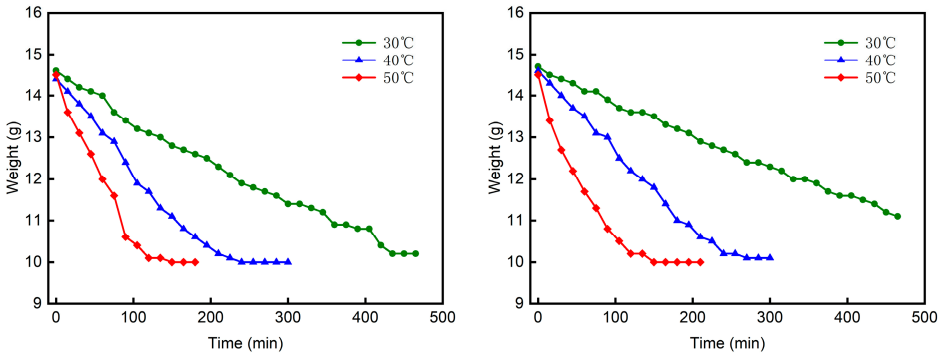


(**a**) Straight-blade (**b**) Tri-blade

**Figure 7.** Weight changes during the coating drying process.

The graphs in Figure 7 demonstrate that drying pace is significantly influenced by temperature. An accelerated procedure of drying can be identified by higher temperatures and a faster rate of weight loss. However, weight loss happens more gradually at lower temperatures, which would point to a delayed drying process. The data shows that as drying temperature rises, so does the rate of weight loss. This makes sense because higher temperatures have been associated with rougher and more fractured surfaces, whereas a quicker process of drying may lead to defects that show up earlier. As the drying temperature rises, the time required for the coating to reach complete dryness decreases rapidly. A very fast drying rate can increase internal stress in the coating during the drying process. Additionally, the reduced flowability of the coating at higher temperatures contributes to an increased number of surface cracks.

To balance dehydrating duration and adherence to quality, proper drying conditions must be carefully selected. Extremely high temperatures can speed up drying but may introduce defects underneath the coating, while lower temperatures may delay drying and improve surface smoothness. Thus, for the purpose of improving the application of coatings in manufacturing environments, it is vital to understand the relationship between drying temperatures and coating performance.

## 4. Conclusions

This study investigates the effects of blade shape, stirring speed, stirring time, and drying temperature on the properties of lost foam coatings. The findings are summarized as follows:

(1) The shape of the stirring blade significantly impacts the uniformity, viscosity, and coating weight. The tri-blade configuration achieved the highest mixing efficiency, resulting in consistent viscosity and optimal coating weight. In contrast, the two-blade and serrated blades produced less-uniform mixtures, affecting the final coating quality.

(2) Increasing the stirring speed from 800 rpm to 1200 rpm slightly reduced the viscosity and coating weight due to shear thinning effects. However, the overall change was minimal, indicating effective mixing within this speed range.

(3) Extending the stirring time beyond 30 min did not significantly alter the coating's viscosity or application weight. A stirring time of 30 min was sufficient to achieve stable properties, with prolonged stirring offering no substantial improvements.

(4) Higher drying temperatures increased surface cracking and roughness. Coatings dried at 50 °C exhibited the most significant defects, while those dried at room temperature were smoother with fewer cracks. Thus, controlling the drying temperature is crucial for minimizing surface imperfections and ensuring high-quality coatings.

**Author Contributions:** Conceptualization, G.S.; methodology, G.S., Z.L. and Q.W.; formal analysis, G.S., Q.W. and Z.L.; investigation, G.S., Q.W. and Z.L.; data curation, G.S., and Q.W.; writing—original draft preparation, G.S.; writing—review and editing, G.S. and Z.L.; supervision, G.S. and Z.L. All authors have read and agreed to the published version of the manuscript.

**Funding:** The authors acknowledge financial support from Kunlun Talent Project of Qinghai Province (2023-QLGKLYCZX-034).

**Institutional Review Board Statement:** Not applicable.

**Informed Consent Statement:** Not applicable.

**Data Availability Statement:** Data are contained within the article.

**Acknowledgments:** We thank Xiaoming Liu for his contribution to the paper.

**Conflicts of Interest:** The authors declare that they have no known competing financial interests or personal relationships that could have appeared to influence the work reported in this paper.

## References

1. Kay, A. Vacuum precision investment casting for clean metal castings. *Foundry Trade J.* **2006**, *180*, 280–282.
2. Zhu, H.C.; Zhang, R.; Li, H.B.; Jiang, Z.H.; Zhang, S.C.; Geng, Y.F. Evolution of Temperature Field of Slabs during the Feeding Strip Process in Continuous Casting. *Steel Res. Int.* **2023**, *94*, 2300031. [CrossRef]
3. Jiang, Z.; Fan, Z.; Jiang, W.; Li, G.; Wu, Y.; Guan, F.; Jiang, H. Interfacial microstructures and mechanical properties of Mg/Al bimetal produced by a novel liquid-liquid compound casting process. *J. Mater. Process. Technol.* **2018**, *261*, 149–158. [CrossRef]
4. Santa-Rosa, W.; Venet, M.; M'Peko, J.C.; Moreno, R.; Amorín, H.; Algueró, M. Environmentally-friendly magnetoelectric ceramic multilayer composites by water-based tape casting. *J. Eur. Ceram. Soc.* **2019**, *39*, 1065–1072. [CrossRef]
5. Schulz, T.; Janke, D.; Heller, H.P.; Lychatz, B. Development of environmentally friendly continuous casting fluxes. *Stahl Und Eisen* **2008**, *128*, 65–78.
6. Scarber, P.; Littleton, H.; Druschitz, A. Preliminary Study of Compacted Graphite Iron Engine Blocks Produced by the Lost Foam Casting Process. *Trans. Am. Foundry Soc.* **2009**, *117*, 889-881.
7. Druschitz, A.; Littleton, H.; Dunlap, W.; Foley, R.; Schroeder, T.; Reynolds, J.; Harvey, B. Advantages of pouring compacted graphite iron using the lost foam casting process. *Int. Foundry Res.* **2012**, *64*, 577–583.
8. Kiran, S.B.; Krishna, R.; Bhanuprakashreddy, D.; Divya, M.; Yadav, A.; Suresh, P.; Rao, T.V.V.L.N.; Colak, I. Structural analysis of grey iron nose leg component produced by lost foam casting. In *AIP Conference Proceedings*; AIP Publishing LLC: Long Island, NY, USA, 2023.
9. Bieniewicz, K.; Reich, M.; Soraruf, N. Improving Metal Flow in LOST FOAM CASTING Through Use of Low Thermal Degradation Hot Melt Adhesives. *Mod. Cast.* **2024**, *114*, 36–44. [CrossRef]
10. Kavitha, M.; Raja, V. Optimization of insert roughness and pouring conditions to maximize bond strength of (Cp)Al-SS304 bimetallic castings using RSM-GA coupled technique. *Mater. Today Commun.* **2024**, *39*, 108754. [CrossRef]
11. Romazanov, Z.; Silayeva, O.; Tatieva, M.L.M.P.A. The feasibility study for the creation of production based on technology of lost-foam casting. *Metalurgija* **2023**, *62*, 103–106.
12. Shabestari, S.G.; Divandari, M.; Ghoncheh, M.H.; Jamali, V. Interplay among Coating Thickness, Strip Size, and Thermal and Solidification Characteristics in A356 Lost Foam Casting Alloy. *Metall. Mater. Trans. B* **2017**, *48*, 2304–2315. [CrossRef]
13. Jiao, C.; Li, G.; Tian, L.; Chen, S.; Kang, C.; Sun, G. Preparation and properties of magnesia porous ceramics by particle-stabilized foam casting. *Int. J. Appl. Ceram. Technol.* **2023**, *20*, 2985–2992. [CrossRef]
14. Cibikci, K.C.; Yaman, M. Experimental investigation of compressive behavior and vibration properties of layered hybrid foam formed by aluminum foam/EPS-filled syntactic foam. *J. Mater. Sci.* **2024**, *59*, 3636–3651. [CrossRef]
15. Acar, S.; Gecü, R.; Kisasöz, A.; Güler, K.A.; Karaaslan, A. A Study on Al/Cu Bimetal Production by Lost Foam Casting. *Pract. Metallogr.* **2018**, *55*, 728–740. [CrossRef]

16. Huang, J.; Lin, Y.X.; Chen, W.P.; Qi, X.J. Numerical analysis of lost foam casting for large-caliber water meter shell. *Adv. Mech. Eng.* **2021**, *13*, 168781402110280. [CrossRef]
17. Griffiths, W.D.; Davies, P.J. The permeability of Lost Foam pattern coatings for Al alloy castings. *J. Mater. Sci.* **2008**, *43*, 5441. [CrossRef]
18. Akbarzadeh, Y.; Rezaei, M.; Babaluo, A.A.; Charchi, A.; Azimi, H.R.; Bahluli, Y. Microstructure, permeability and rheological behavior of lost foam refractory coatings. *Surf. Coat. Technol.* **2008**, *202*, 4636–4643. [CrossRef]
19. Karimian, M.; Idris, M.H.; Ourdjini, A.; Muthu, K. Effect of flask vibration time on casting integrity, Surface Penetration and Coating Inclusion in lost foam casting of Al-Si Alloy. *Eur. J. Pharmacol.* **2011**, *1315*, 633–638.
20. Sands, M.; Shivkumar, S. Influence of coating thickness and sand fineness on mold filling in the lost foam casting process. *J. Mater. Sci.* **2003**, *38*, 667–673. [CrossRef]
21. Opyd, B.; Granat, K. Evaluation of Microwave Heating of Protective Coatings Used in the Lost Foam Technology. *Arch. Foundry Eng.* **2015**, *15*, 65–70. [CrossRef]
22. Shivkumar, S.; Yao, X.; Makhlouf, M. Polymer Melt Interactions During Casting Formation in the Lost Foam Process. *Scr. Metall. Mater.* **1995**, *33*, 99227. [CrossRef]
23. Holtzer, M.; Bobrowski, A.; Drożyński, D.; Mocek, J. Investigations of Protective Coatings for Castings of High-Manganese Cast Steels. *Arch. Foundry Eng.* **2013**, *13*, 39–44. [CrossRef]
24. Sun, C.; Cao, Z.; Liu, G. Effect of refractory aggregate shape on the porosity of A356 alloy castings in lost foam casting. *Int. J. Met.* **2024**, *18*, 2499–2507. [CrossRef]
25. Pavlović, M.; Nikolić, J.; Andrić, L.; Todorović, D.; Bozić, K.; Drmanić, S. Synthesis of the new lost foam refractory coatings based on talc. *J. Serbian Chem. Soc.* **2021**, *87*, 491–503. [CrossRef]
26. Sulaiman, S.; Ariffin, M.K.A.M.; Tang, S.H.; Saleh, A. Influence of Pattern Coating Thickness on Porosity and Mechanical Properties of Lost Foam Casting of Al-Si (LM6) Alloy. *Appl. Mech. Mater.* **2013**, *300–301*, 1281–1284. [CrossRef]
27. Pimenta, J.T.; Gonçalves, C.; Hiliou, L.; Coelho, J.F.; Magalhaes, F.D. Effect of binder on performance of intumescent coatings. *J. Coat Technol. Res.* **2016**, *13*, 227–238. [CrossRef]
28. Marefat Seyedlar, R.; Imani, M.; Mirabedini, S.M. Intumescent coatings based on polyfurfuryl alcohol: A design-of-experiments approach. *Polym. Bull.* **2024**, *81*, 8229–8250. [CrossRef]
29. Chang, A.S.; Jang, T.Y.; Shih, T.S. The strength of coating in the lost foam casting process. *Int. J. Cast Met. Res.* **2000**, *12*, 251–261. [CrossRef]
30. Sun, C.; Cao, Z. Effects of the Wettability Between the Coating and the Liquid EPS on the Filling Process of Lost Foam Casting. *Int. J. Met.* **2024**, *18*, 1318–1328. [CrossRef]
31. Guler, K.A.; Kisasoz, A.; Karaaslan, A. Effects of pattern coating and vacuum assistance on porosity of aluminium lost foam castings. *Russ. J. Non-Ferr. Met.* **2014**, *55*, 424–428. [CrossRef]
32. Tuttle, R.; Ramrattan, S.; Wells, L. As-Cast Surface Characterization for Steel Using Disk-Shaped Chemically Bonded Sand Specimens. *Int. J. Met.* **2021**, *15*, 382–390. [CrossRef]
33. Gao, Y.X.; Zhao, C.; Fang, Z.G.; Yi, J. Microstructures and Wear Properties of Micro-Nanostructure Coating on Cast Iron Rolls by Electro-Spark Deposition. *Adv. Mater. Res.* **2011**, *160–162*, 176–181. [CrossRef]